Damage Identification based on Vibration Measurements Applied to Masonry Structures

Luís F. Ramos,
University of Minho, Department of Civil Engineering,
Campus de Azurém, 4800-058 Guimarães, Portugal
e-mail: **lramos@civil.uminho.pt**

Guido de Roeck,
K.U.Leuven, Department of Civil Engineering, Belgium

Paulo B. Lourenço and
University of Minho, Department of Civil Engineering, Portugal

Alfredo Campos-Costa
LNEC, Lisbon, Portugal

Abstract

The present paper aims to explore damage assessment in the masonry structures at an early stage by vibration measurements. Two replicates of historical constructions were built in virgin state: one arch with 1.5 m span and one shear wall with 1.0 m^2. Afterwards, progressive damage was applied and sequential modal identification analysis was performed at each damage stage, aiming to find adequate correspondence between dynamic behavior and internal crack growth. Accelerations and strains in many points were record in the replicates. Eigen frequencies, mode shapes and modal strains were derived from the dynamic measurements. Environmental effects of the temperature and relative humidity on the dynamic response were studied. A first updating process was performed on the results of the undamaged arch to tune a finite element model. Moreover, the tests were repeated with added masses to scale the mode shapes. Finally, a brief analysis of the results of the several damage scenarios are presented in the paper

1   Introduction

Preservation of the architectural heritage is considered a fundamental issue in the cultural life of modern societies. Modern requirements for an intervention include reversibility, unobtrusiveness, minimum repair and respect of the original construction, as well the obvious functional and structural requirements.

In the process of preservation of ancient masonry structures, damage evaluation and monitoring procedures are particularly attractive, due to the modern context of minimum repair and observational methods, with iterative and step-by-step approaches. High-priority issues related to damage assessment and monitoring are global non-contact inspection techniques, improved sensor technology, data management, diagnostics (decision making and simulation), improved global dynamic (modal) analysis, self-diagnosing / self-healing materials, and improved prediction of early degradation.

It is known for a long time that service loads, environmental and accidental actions may cause damage to the structural systems. In this issue the long life maintenance plays an important roll. Regular inspections and condition assessment of engineering structures allow programmed repair works and economic management of the infrastructures, with significant attenuation on the costs. Relating these aspects to the historical constructions area, maintenance is even more essential because of their cultural importance of

these constructions, the safety of visitors, potential seismic risk and the accumulation of physical, chemical and mechanical damage through the time.

Alterations of geometrical dimensions, boundary conditions and mass, and the degradation of the mechanical properties of the materials, including physical damage, or the simultaneously occurrence of all these phenomena, affect the dynamic behavior of the structures, i.e. change the resonant frequencies, mode shapes, damping coefficients and the quantities derived from the basic modal parameters, see [1]. If the environmental influence (temperature, moisture, etc) is evaluated and separated from the dynamic response of the structure, see [2], the damage occurrence can be globally detected. After detection, next task is to localize the damage and its extension with more detail. Finally, its consequences for the construction should be evaluated. As far as concerned to masonry constructions, there are few references in literature dedicated to damage identification based on vibration signatures.

2   Damage Identification Process

The present paper tries to deal with the problem of damage identification by using Global and Local damage identification techniques. It is advantageous to have two categories of damage assessment methods: (a) the vibration based damage identification methods, currently defined as Global methods, because they do not give sufficiently accurate information about the extent of the damage, but they can alert its presence and define the precise location of it (e.g. [3]); and (b) the methods based on visual inspections through or experimental tests like acoustic or ultrasonic methods, magnetic field methods, radiograph, eddy-current methods and thermal field methods (e.g. [4]), also called as Local methods. The last ones need the preceding global approach (Global methods) to detect and localize the damage, and then, if the possible location of damage is accessible in the structure, they can describe the damage in an accurate way.

From another point of view, to study more carefully the damage identification problem, in [5] is underlined the importance of using exact taxonomy for the precise definition of what constitutes a fault, a damage and a defect in a structure. The authors proposed the following definitions:

- **Fault** is a state when the structure can no longer operate satisfactorily, caused by an unacceptable reduction in the quality for user requirements;

- **Damage** is when the structure is no longer operating in its ideal condition, but can still function satisfactorily;

- **Defect** is inherent in the material and statistically all materials have some unknown amount of defects. This means that the structure can operate in its ideal condition even if the materials contain defects.

The definition above allows a hierarchical relationship: defects can leads to damage and damage leads to fault. This relationship can be used to establish a state when the presence of several damages scenarios means that the structures can no longer operating in a satisfactory manner.

In the literature of vibration based damage identification methods it is common by assume that damage is directly related to a decrease of stiffness and not to any change of the mass. The next step of the methodology for damage identification is to define a classification for the methods and actions used in the process of monitoring and accessing the damage. The first historic classification was presented in [6] where four levels of damage assessment (classical definition) were established:

- **Detection** (Level 1): the method gives a qualitative indication that damage might be present in the structure;

- **Localization** (Level 2): the method gives information about the probable position of the damage;

- **Assessment** (Level 3): the method gives an estimate of extent of the damage;

- **Prediction** (Level 4): the method offers information about the safety of the structure, estimating the residual operating life.

Each presented level is connected in a hierarchical way, because to pass for the following level it is necessary to know the previous one. It is also stressed that the term damage identification is the conjunction of one ore more presented levels.

More recently, in [5] a classification with one inter-mediate level is proposed leading to the following levels:

- **Detection** (Level 1): the method gives a qualitative indication that damage might be present in the structure;

- **Localization** (Level 2): the method gives information about the probable position of the damage;

- **Classification** (new Level 3): the method gives information about the type of dam-age;

- **Assessment** (new Level 4, the classical Level 3): the method gives an estimate of the extent of the damage;

- **Prediction** (new Level 5, the classical Level 4): the method offers information about the safety of the structure, estimating the residual operating life.

In author's opinion, the introduction of the third level is vital for effective identification of Level 5 (classical Level 4) and possibly for Level 4 (classical Level 3), since information about the characteristics of damage is necessary to predict the residual operating life time of the structure. Also, all the first four levels need structural observation while the last one can be estimated by numerical analysis.

The Global vibration methods can be divided by Linear or Nonlinear depending on which type of behavior is assumed after the damage occurrence. If during the dynamic test the crack is assumed to remain open, the response is linear and the method is classified as Linear. In this last classification, the damage can be only associated with changes in boundary conditions, material properties (loss of stiffness) or changes in geometry. On the contrary, the Nonlinear methods take into account the changing stiffness according with the oscillating amplitudes for the simulation of the crack breathing, i.e. when the crack is closed there is a restoration of the original stiffness, see Figure 1. The Linear methods are often founded in literature. They can also be divided as Model Based or Non-model Based methods, depending whether or not they use numerical models for the damage identification.

(a)   (b)   (c)

Figure 1: Crack breathing of a cantilever beam: (a) crack closed with restoration of the initial stiffness; (b) transitory stage; and (c) crack open with minimum stiffness

Related to the last issue, in the present work it is assumed that the modal identification can be accurately performed with linear modal analyses at very low ambient excitation level. Cracks breathing effects will not occur or they will be small.

3   Vibration based Damage Identification Methods

There is not yet one methodology which gives accurate damage identification through all the presented levels of damage assessment and for all type of structural systems. So, it is still a challenge for the next decades [7]. In literature it exists a number of papers which summarize the principal developments in this field (see [1]; [3], [7]; [8] and [9]).

4   Application to Masonry Constructions

As previously mentioned, there are few references in literature where damage identification based on dynamic response is applied to masonry structures. The first attempt at the University of Minho to establish a relation between the damage progress and the dynamic response of a masonry building was done on a real scale rubble stone masonry structure (see Figure 2), built in the "Laboratório Nacional de

Engenharia Civil" (LNEC), at Lisbon. This structure was tested in the LNEC shake table, under the EU RP within the 5th EU framework program, ECOLEADER – Enhancing Seismic Resistance and Durability of Natural Stone Masonry.

In the works of ECOLEADER Project several and progressive damage scenarios were induced in the shaking tests. At each scenario, a modal identification was performed with operational modal analysis techniques for further comparison between each damage scenario and the virgin stage of the structure. The results of this study are presented elsewhere [10]. The natural frequencies decreased significantly during the several damage scenarios, see Table 1, but the relation between the dynamic response and the crack pattern was difficult to analyze. Furthermore it was decided to study simpler models and two masonry replicates were constructed in the Laboratory of University of Minho, which is the main focus of the present paper.
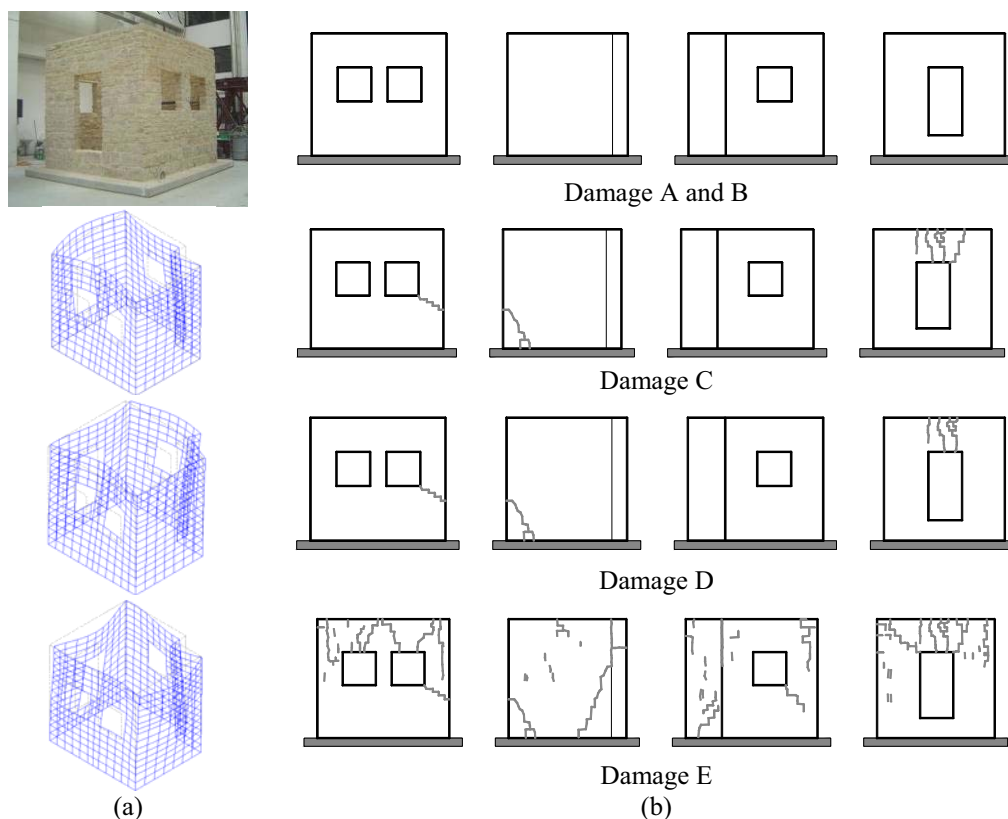

Figure 2: Masonry mock-up: (a) general view and the first three numerical mode shapes; and (b) the progress of the crack pattern along the several damage stage

Mode Shape	Damage Stage				
	A	B	C	D	E
1st	15.05	12.28	10.60	7.55	4.62
2nd	19.79	13.97	12.29	9.60	6.13
3rd	20.50	18.30	16.63	12.96	8.71
4th	26.57	21.27	17.60	13.83	12.80
5th	28.91	25.94	19.56	17.58	13.61
6th	36.85	32.87	28.06	23.82	15.40
7th	39.73	33.69	32.06	28.99	21.64

Table 1: Frequencies decreasing along the damage scenarios

5   Tests of the Masonry Replicates in Laboratory

The two replicates of ancient masonry arches and walls were built with clay bricks and poor mortar joints, see Figure 3. Progressive and controlled damage was applied by static loads. On each model it was intended to reach multiple damage levels (several cracks). Between each stage, modal identification

analysis using output-only (ambient or natural vibration) techniques was done, where the ambient temperature and humidity were also recorded, to evaluate small environmental changes on the dynamic response of the specimen. The modal identification tests at each load stage/damage scenario were performed by two different excitation conditions: natural ambient noise present in the laboratory and random excitation in space and time, induced by an impact hammer (2.5 kg of mass). The produced impact forces were about 5% of the mass of the models.
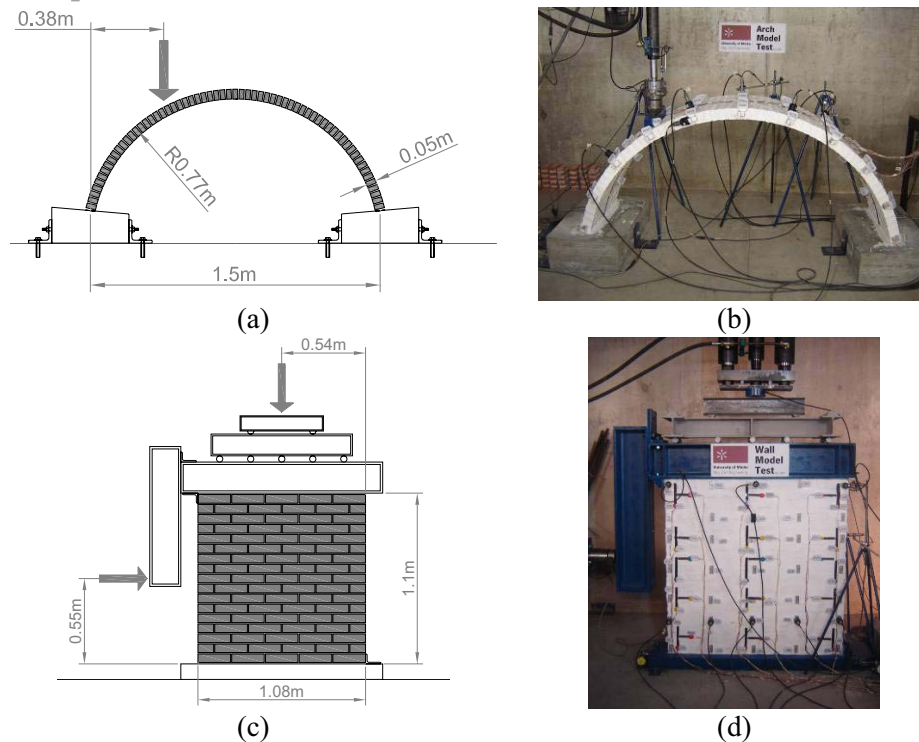

Figure 3: Masonry replicates: (a) and (b) the arch model; and (c) and (d) the wall model

5.1 Test Planning and Analysis Procedures

For each model several damage scenarios were induced by static loads on the specimen (see Figure 3). Figure 5 shows the response of the models during the subsequent static tests and some crack patterns in the specimen. Following each stage it was possible to observe the decrease of the stiffness. The maximum crack openings were 0.05 and 1.20 mm for the arch and wall models, respectively. Between each stage, at unloading, it was difficult to visually observe the cracks.

On each model, both accelerations and strains were recorded. The acceleration response of the arch was measured in twenty-two points, equally distributed along the two longitudinal edges of the vault and in the arch plane directions. The response of the wall was measured in a regular net of thirty-five points and in the out of plane direction. The strains in both models were measured with quarter bridge configurations and they were disposed in a way to measure the curvature mode shapes. The mesh of sensors was kept rather close to have better resolution in the higher mode shapes. Thus, the maximum distance between sensors was 20 cm, approximately 1/8 of their maximum dimension.
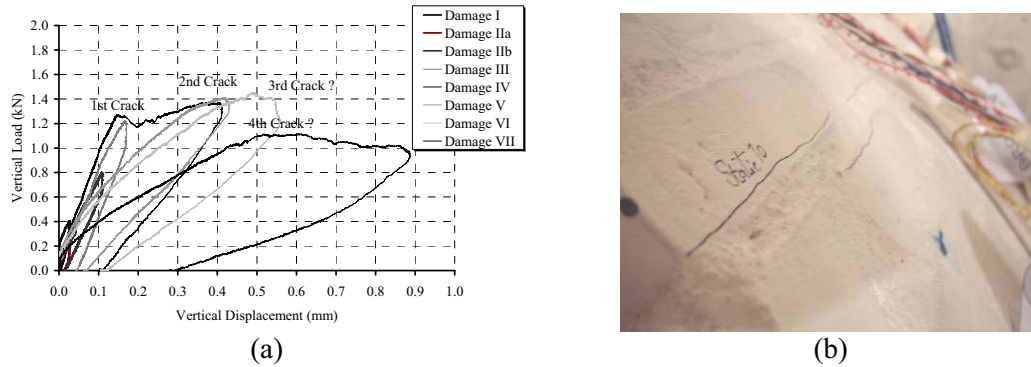
Figure 4: Arch model damage scenarios: (a) static test; and (b) one crack with 0.05 mm width
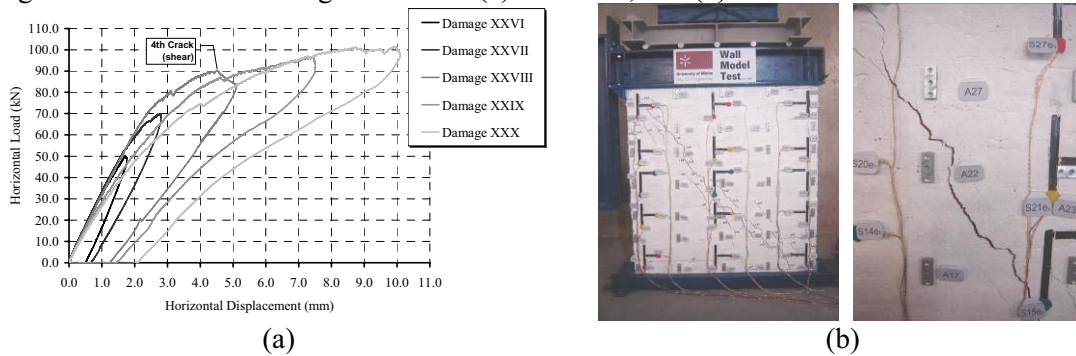

Figure 5: Wall model damage scenarios: (a) static test; and (b) one crack with 1.20 mm width

The acquisition system was composed by 8 uniaxial piezoelectric accelerometers, with a bandwidth ranging from 0.15 to 1000 Hz (5%), a dynamic range ±0.5 g and a sensitivity of 10 V/g, and several strain gauges of 120 Ω resistance. They were connected to a data acquisition system with 16 bit A/D converter, and anti-aliasing filters for both strains and accelerations.

In the analysis of each model, the modal parameter estimation was done with Stochastic Sub-space Identification (SSI) techniques. These techniques are suited for systems under natural (ambient or operational) conditions, and they are based on the assumption that the excitations are reasonably random in time and in the physical space of the structure [11], [12].

For the damage identification process a selected group of damage detection methods presented in literature, see [1] and [13], will be used to validate their performance for Levels 1 and 2. The selected methods will be the Damage Index Method and the Direct Stiffness Calculation applied to shell alike structures.

In a second and more detailed phase, model updating techniques presented in [14] will be performed. This belongs to another group of damage assessment methods, where a finite element model is calibrated for every damage stage by minimizing the differences between calculated and measured modal parameters.

5.2   Preliminary Results

At the moment only some data from the extensive test campaign was analyzed. In this paper some preliminary results will be reported: (a) comparison between the results of different SSI techniques applied to the arch reference tests in the undamaged condition, (b) the influence of the ambient temperature and the humidity in the laboratory, (c) first attempt of model updating, (d) results from the tests with added masses to scaled the modes shapes and (d) the evolution of the natural frequencies between the several damage scenarios.

5.2.1   Comparison between Different SSI Techniques

The SSI techniques selected were the Principal Component method available in the ARTeMIS Extractor software [15] and the SSI/Ref method in the MACEC tool implemented in MatLab by the Catholic

University of Leuven [16]. The results were accurate and are satisfactory for both analyses. Seven mode shapes were easily estimated with ambient and randomly distributed impact tests. Figure 6 shows the estimated mode shapes by the two softwares.

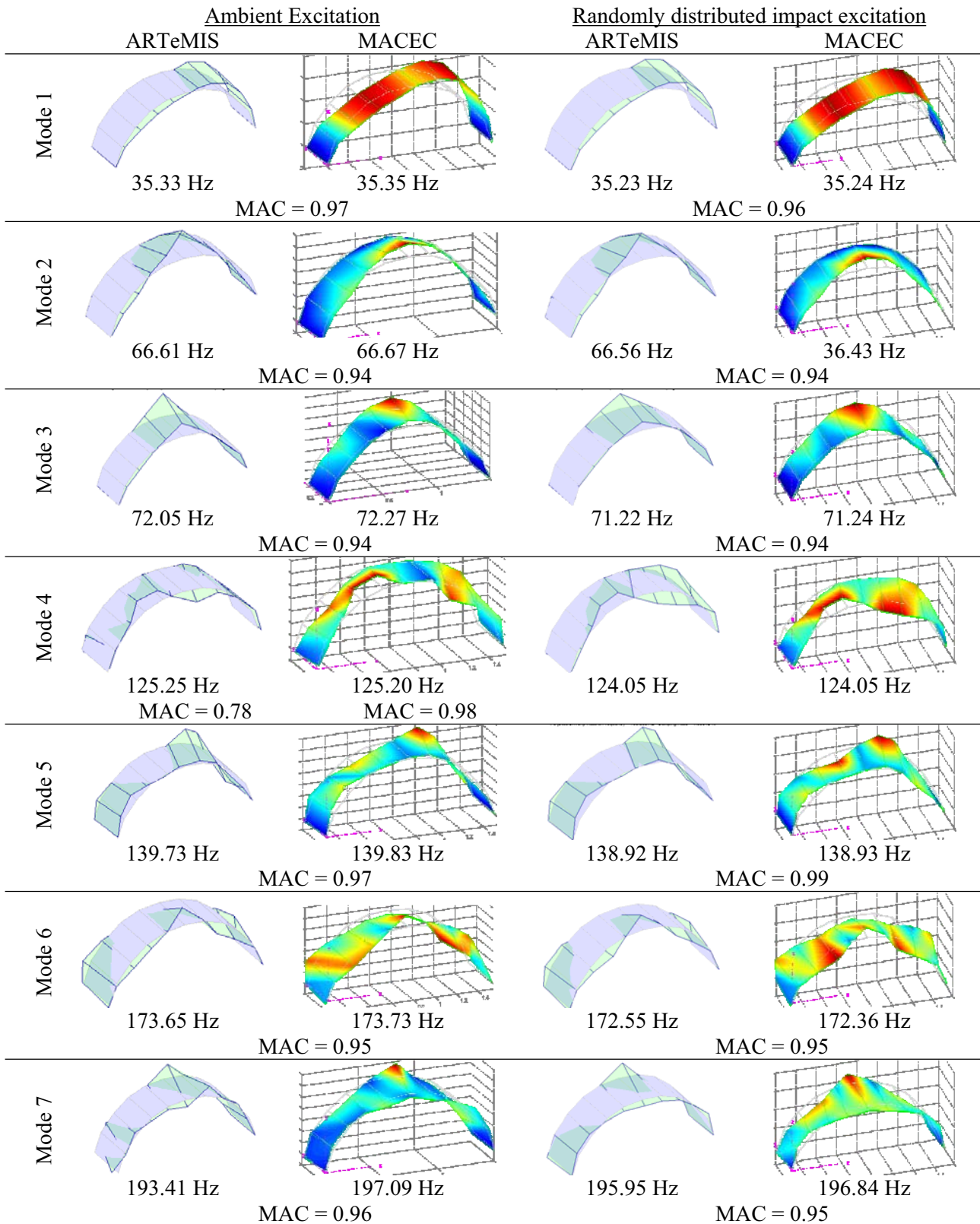|	Ambient Excitation		Randomly distributed impact excitation	
	ARTeMIS	MACEC	ARTeMIS	MACEC
Mode 1	35.33 Hz	35.35 Hz	35.23 Hz	35.24 Hz
		MAC = 0.97		MAC = 0.96
Mode 2	66.61 Hz	66.67 Hz	66.56 Hz	36.43 Hz
		MAC = 0.94		MAC = 0.94
Mode 3	72.05 Hz	72.27 Hz	71.22 Hz	71.24 Hz
		MAC = 0.94		MAC = 0.94
Mode 4	125.25 Hz	125.20 Hz	124.05 Hz	124.05 Hz
	MAC = 0.78	MAC = 0.98		
Mode 5	139.73 Hz	139.83 Hz	138.92 Hz	138.93 Hz
		MAC = 0.97		MAC = 0.99
Mode 6	173.65 Hz	173.73 Hz	172.55 Hz	172.36 Hz
		MAC = 0.95		MAC = 0.95
Mode 7	193.41 Hz	197.09 Hz	195.95 Hz	196.84 Hz
		MAC = 0.96		MAC = 0.95

Figure 6: Mode shape configurations for all the analyses in virgin stage

Table 2 summarizes the results comparing the frequencies values and the mode shapes configuration through the Modal Assurance Criterion (MAC) values. It is stressed that the results are highly accurate for frequencies and modal displacements, as the error between the resonant frequency values is less than 2% and the MAC values are greater than 0.94. The damping values were depending on the excitation mechanism, but an average value of 0.6% can be observed for all modes and all analyses. Furthermore, the damping will be not used for the damage detection analysis.

| Modes | Ambient Excitation | | | | Randomly Distributed Impact Excitation | | | |
	ARTeMIS Hz	MACEC Hz	Error %	MAC	ARTeMIS Hz	MACEC Hz	Error %	MAC
1	35.33	35.35	0.05	0.97	35.23	35.23	0.01	0.97
2	66.61	66.67	0.09	0.94	66.56	66.43	0.19	0.95
3	72.05	72.27	0.31	0.94	71.22	71.24	0.02	0.94
4	125.25	125.20	0.04	0.78	124.05	124.05	<0.01	0.98
5	139.73	139.83	0.07	0.97	138.92	138.92	<0.01	0.99
6	173.65	173.73	0.04	0.95	172.55	172.38	0.10	0.95
7	193.41	197.09	1.90	0.96	195.95	196.83	0.44	0.95

Table 2: Results comparison between different SSI analyses

As strains were measured on 11 points in the extrados and intrados of one median line along the arch, it was also possible to estimate the curvature mode shapes of the specimen. The curvatures were only possible to estimate with accuracy in the case of randomly distributed impact excitation tests, because with ambient vibration excitation the signal to noise ratio was too small.
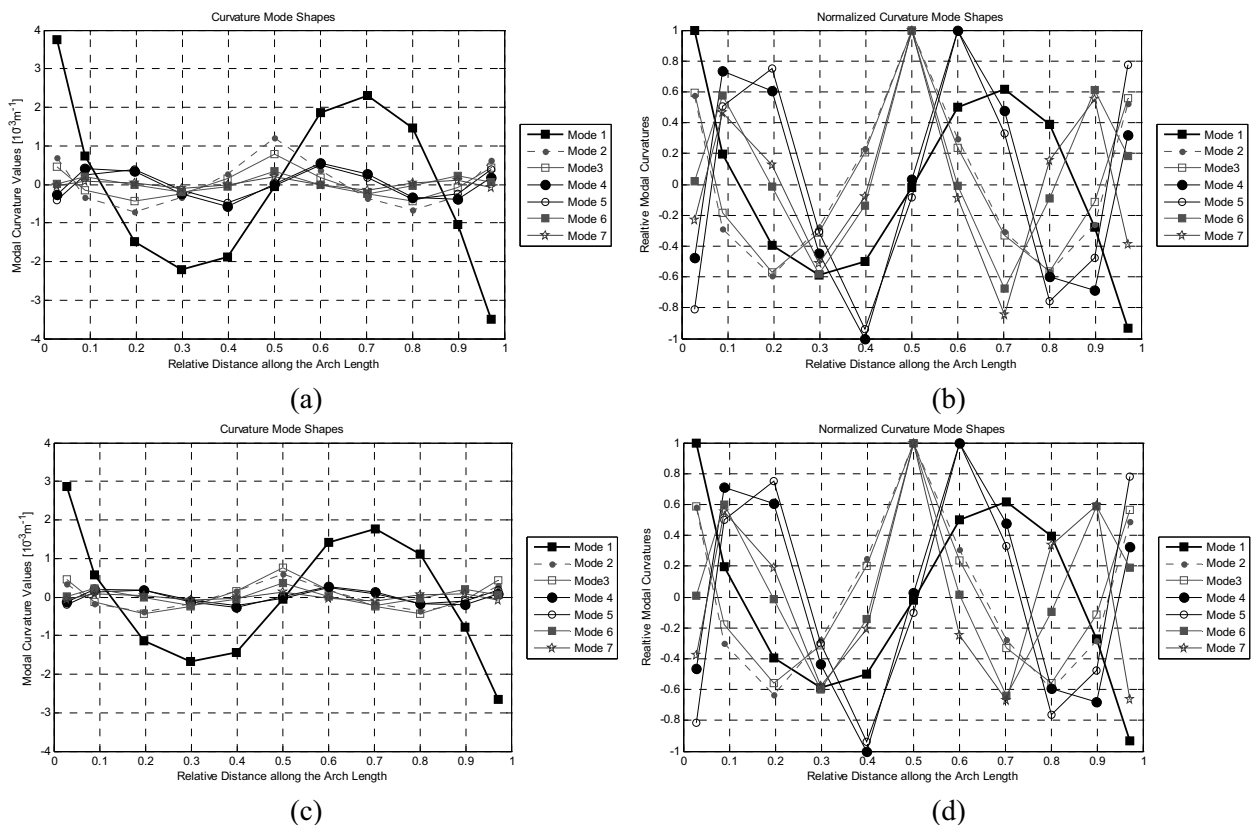

Figure 7: Curvature mode shapes estimated by the two techniques along the normalized arch length: (a) and (b) estimated with ARTeMIS; and (c) and (d) estimated with MACEC

In the left side of Figure 7 is possible to observe the modal curvatures with the same normalization of the modal displacements (i.e. the maximum real value of the modal displacement is equal to 1) and at the right side the modal curvatures normalized to the maximum real value of the modal curvatures. In Figure 7b and d the symmetry or anti-symmetry of the modal curvatures along the arch is stressed. The modal curvatures will be valuable quantities for subsequent damage analysis, since if the Euler-Bernoulli

hypothesis is assumed, the bending stiffness and also the normal stiffness are directly related to the curvatures and the average strains in the arch, respectively.

5.2.2 Temperature and Humidity Effects in the Laboratory

To investigate the possible environmental influence of the temperature in the laboratory and also relative air humidity, a series of tests was performed to evaluate the influence of those parameters. Due to daily variations of heating and ventilation in the laboratory it was observed that the temperature could change 3ºC in one hour (the approximate time of one entire group of test setups per specimen). Therefore, an induced temperature variation with some heating devices positioned close to the arch was performed (see Figure 8a).
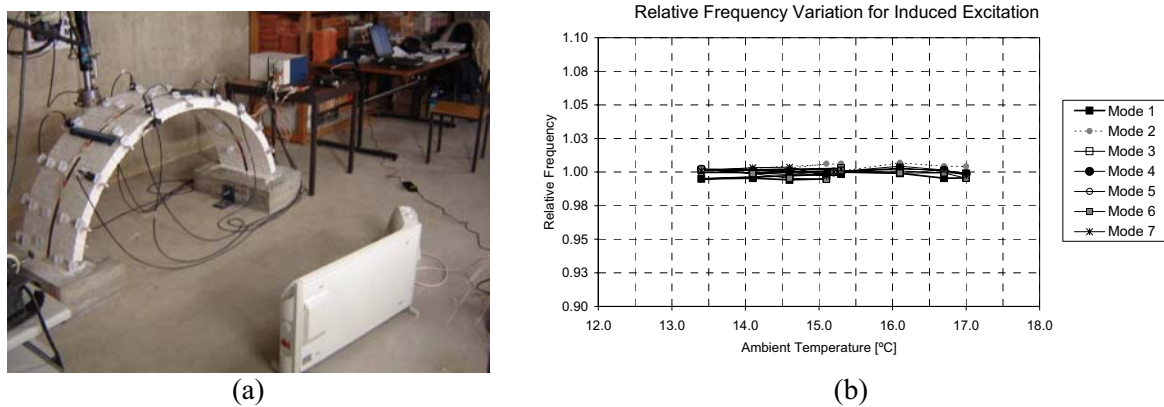

| (a) | (b) |

Figure 8: Temperature test in the arch model: (a) test apparatus; and (b) relative frequency variation according to the ambient temperature

Ambient and surface temperatures and relative air humidity percentage values were recorded. Figure 8b and Table 3 present the results. It is observed that the environmental effects on the dynamic response can be neglected. These tests also show the reliability and repetitivity of the frequency measurements according to CV values which are lower than 0.28%.

Test	Environmental Parameters			Resonant frequencies [Hz]						
	Ambient [ºC]	Surface [ºC]	Humidity [%]	1st	2nd	3rd	4th	5th	6th	7th
1	15.20	16.00	43.10	35.18	65.98	70.76	123.86	138.43	172.52	195.76
2	16.10	16.20	45.00	35.14	66.43	70.97	124.15	138.54	172.39	196.62
3	16.70	16.80	46.00	35.02	66.26	70.82	124.03	138.38	172.41	196.04
4	17.00	17.70	46.80	35.02	66.25	70.69	123.69	138.27	171.72	195.24
5	15.10	16.80	46.60	35.00	66.38	70.58	123.69	138.07	171.56	195.19
6	14.60	16.60	46.00	34.97	66.15	70.63	123.96	138.37	171.73	196.47
7	14.10	16.50	46.20	35.02	66.06	70.71	124.01	138.34	172.31	196.39
8	13.40	15.80	46.00	35.00	66.03	70.86	124.10	138.37	172.92	195.95
9	15.30	16.10	48.70	35.13	66.39	70.97	123.84	138.47	172.76	196.18
$\bar{x}$	15.28	16.50	46.04	35.05	66.21	70.78	123.92	138.36	172.26	195.98
σ	1.18	0.57	1.49	0.07	0.17	0.14	0.17	0.13	0.48	0.51
CV	7.70%	3.47%	3.23%	0.21%	0.25%	0.20%	0.14%	0.10%	0.28%	0.26%

Table 3: Results form the temperature and humidity tests

5.2.3 Preliminary Model Updating

Before any attempt to identify damage, model updating techniques was applied to the arch to assess the dynamic behavior in its undamaged condition. This task was also done to be a first approach in the understanding of the arch behavior. A nonlinear least square method implemented in MatLab was used to

minimize the objective function π, composed by the residuals formed with calculated and experimental frequencies and mode shapes, given by:

$$\pi = \frac{1}{2}\sum_{i=1}^{m}\left[W\left(\left(\frac{f_i^2 - f_{i,\exp}^2}{f_{i,\exp}^2}\right)^2 + \sum_{j=1}^{n}\left(\varphi_{ij} - \varphi_{ij,\exp}\right)^2\right)\right] \tag{1}$$

where m denotes the number of eigen frequencies/eigen modes to take in to account, n denotes the number of measured degrees of freedom and W is a weighting diagonal matrix, which introduces the uncertainties in the measurements, similar to what is proposed in [17], by

$$W = \left[diag\left(CV_1, CV_2, ..., CV_m\right)\right]^{-1} \tag{2}$$

where CV is the coefficient of variation ($CV_i = \sigma_i / f_i$) calculated with the standard variation obtained from the several tests setups on the system identification analysis.

In Equation (1) both experimental and numerical mode shapes are normalized in a way that the maximum real value of the model displacement is equal to 1.

The selection of the optimization parameters was done taking into account the geometrical survey of the arch and the unknown material properties of the masonry, where the possible orthotropic behavior was accounted for. The values considered for the parameters are presented in Table 4. One conclusion emerged from the optimization analysis is the fact that the arch response is very sensitive to the geometry. Therefore, closed constrains were applied to the geometrical parameters, to avoid unrealistic results for the final values.

| Updating Parameters	Initial Values	Lower Bound	Upper Bound	Final Values	Difference
E_y [GPa]	3.9000	0.1950	6.4740	3.8000	-0.1000
$P2_x$ [m]	-0.7625	-0.7549	-0.7701	-0.7620	0.0005
$P4_x$ [m]	0.7625	0.7549	0.7701	0.7677	0.0052
$P3_z$ [m]	0.7625	0.7549	0.7701	0.7699	0.0074
$P6_x$ [m]	-0.7650	-0.7574	-0.7727	-0.7709	-0.0059
$P8_x$ [m]	0.7650	0.7574	0.7727	0.7712	0.0062
$P7_z$ [m]	0.7650	0.7574	0.7727	0.7574	-0.0077
Thick [m]	0.0480	0.0408	0.0504	0.0498	0.0018
E_x/E_y	1.2000	0.1200	2.2800	1.0781	-0.1219
Width [m]	0.4500	0.4455	0.4545	0.4545	0.0045
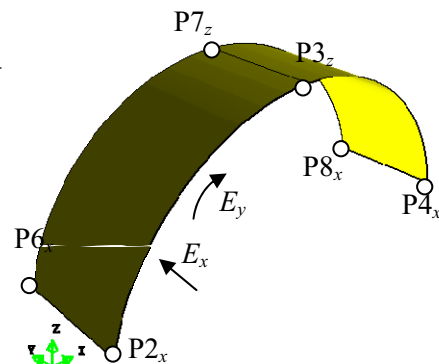
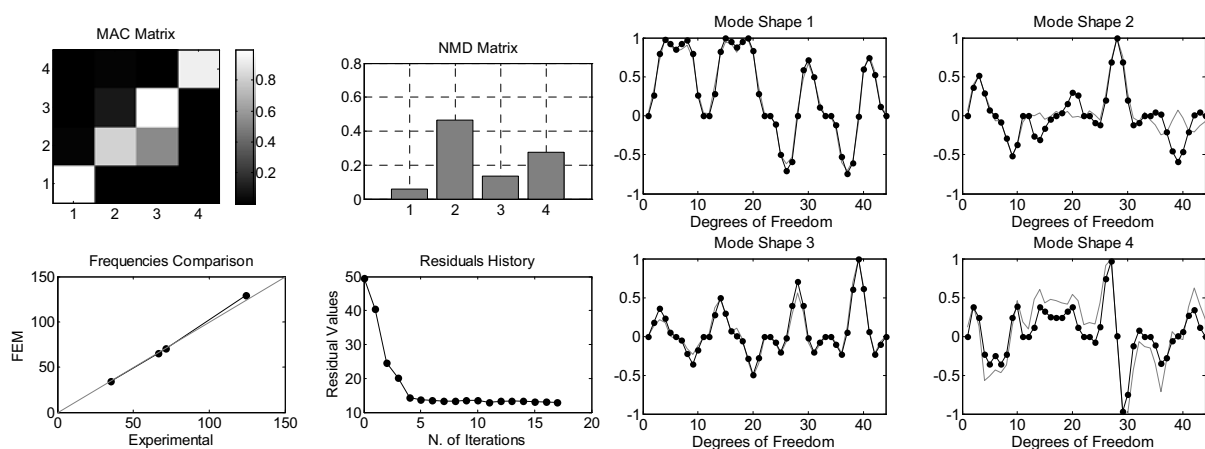Table 4: Optimization parameters and the initial, the restrictions and final values

Figure 9: Results from the optimization analysis

Figure 9 presents the final results from the optimization process, where the first 4 eigen frequencies and 4 eigen modes were included in the objective function. On the figure it is possible to observe the MAC matrix, the Normalized Modal Difference (NMD), the comparison with the measured and calculated

frequencies, the residuals history along the optimization process and the 4 numerical mode shapes compared to the experimental ones.

Table 5 and Figure 10 present the calculated results for the first 7 mode shapes calculated with the optimized parameters presented in Table 4. In terms of frequencies the maximum error is around 8 % for the 6th mode (not included in the objective function). Also high error of 4 and 5% can be founded for the 4th and 5th modes. Concerning the mode shapes (MAC values) there is a good correlation between the experimental and the numerical modal displacements, although the MAC values are less that 0.8 (or NMD values are greater than 0.5) for modes 6 and 7.

Mode	Exp. Freq. [Hz]	σ [Hz]	CV [%]	FEM Freq. [Hz]	Error [%]	MAC	NMD
1st	35.23	0.12	0.33	34.50	2.09	1.00	0.06
2nd	66.43	0.36	0.54	65.27	1.74	0.82	0.47
3rd	71.24	0.21	0.29	70.80	0.62	0.98	0.14
4th	124.05	0.70	0.57	129.13	4.09	0.93	0.28
5th	138.92	0.85	0.61	131.56	5.30	0.95	0.24
6th	172.38	0.92	0.53	186.77	8.35	0.62	0.78
7th	196.83	1.21	0.62	191.54	2.69	0.67	0.70

Table 5: Comparison between experimental and optimized results

Mode 1   Mode 2   Mode 3   Mode 4

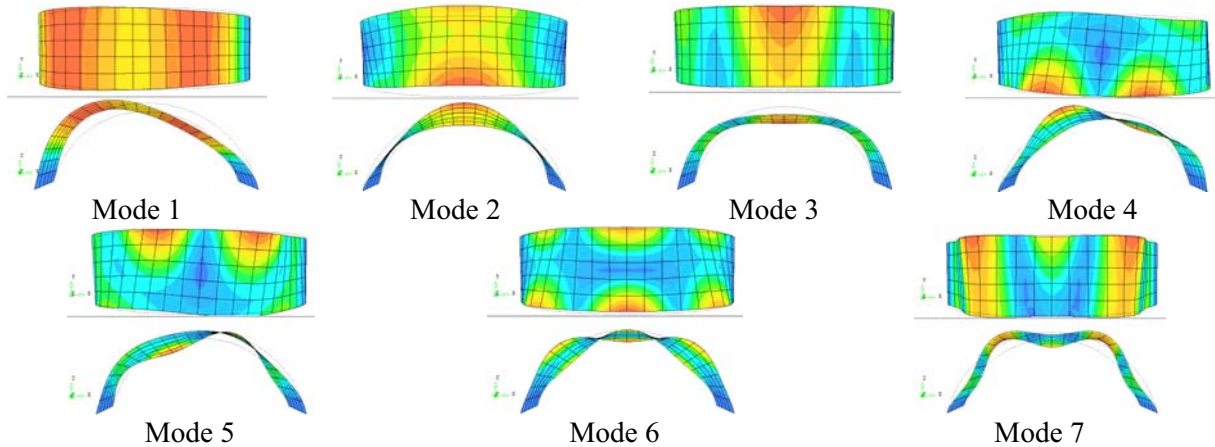Mode 5   Mode 6   Mode 7

Figure 10: Numerical mode shapes (top and lateral views)

The results of this first optimization analysis show that still a better representative of the arch is needed to improve the correspondence between the experimental and the numerical results. Therefore, the Direct Stiffness Calculation (DSC) method presented in [13] will be used to calculate the stiffness distribution along the arch, taking into account the measured curvatures. According to the DSC results, new strategies for the choice of optimization parameters will be followed to obtain even better results.

5.2.4   Mass Scaled Modes

Because some damage identification methods need mass scaled modes and the system identification was done with output-only techniques, the method suggested by [18] was followed to scale the mode shapes.

Two tests were performed, see Figure 11, with approximately 5 and 10% off added masses, uniformly distributed along the arch. The masses were materialized by adding bricks to the top of the arch with plasticine between them to avoid noise contamination in the signals.

The method developed in [18] calculates the scale factors assuming that the shifts in frequencies are small and the modes shapes do not change significantly with the added masses. Therefore, the scale factors can be calculated by the following expression:

$$\alpha_i \approx \sqrt{-\frac{2\Delta\omega_i}{\omega_i \sum_{i=1}^{m} \varphi_i^T \Delta M \varphi_i}} \quad (3)$$

where ω_i are the frequencies and ΔM the added mass matrix according to the added masses in the structure.
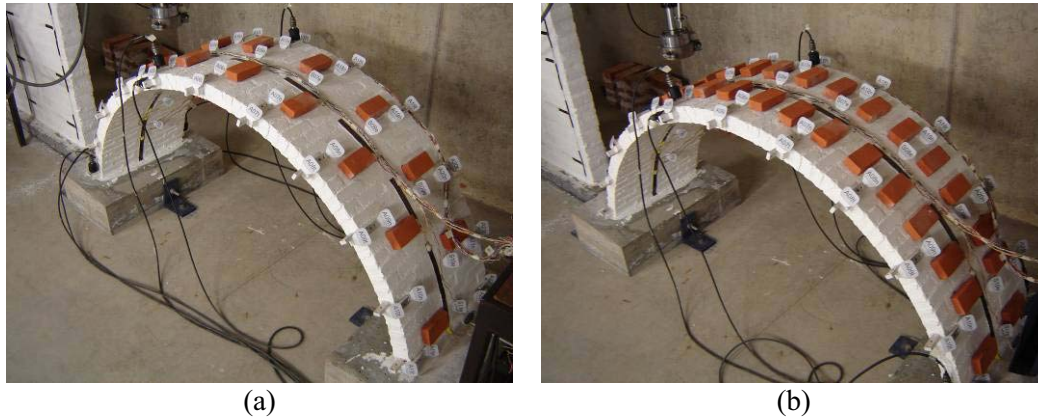

(a)   (b)

Figure 11: Tests for scaling the mode shapes: (a) and (b) with 5 and 10% of added masses, respectively

The results of this technique are presented in Table 6 and they are compared with the scale factors obtained by the FE model presented in the previous section. The differences between the calculated values and the experimental tests are rather small (CV less than 10%). Although, significant errors can be found between numerical and experimental results, especially for higher modes, those with lower MAC values in the optimization analysis. If the results from the model updating analysis will improve by the application of the DSC method, possibly the results from the scaled modes would also improve. Nevertheless, the scale values obtained by the experimental tests seem to be acceptable.

Mode Shape	FEM	Ambient Excitation				Randomly Distributed Impact Excitation			
		5% Mass	Error [%]	10% Mass	Error [%]	5% Mass	Error [%]	10% Mass	Error [%]
1	0.1180	0.0969	17.8	0.1022	13.4	0.1147	2.8	0.1109	6.0
2	0.1802	0.2025	12.4	0.2132	18.3	0.2333	29.5	0.2316	28.5
3	0.2284	0.2592	13.5	0.2433	6.5	0.2357	3.2	0.2235	2.1
4	0.2569	0.1492	41.9	0.1447	43.7	0.1352	47.4	0.1371	46.6
5	0.2577	0.2161	16.1	0.2016	21.8	0.1826	29.1	0.1783	30.8
6	0.2990	0.1134	62.1	0.1367	54.3	0.1213	59.4	0.1240	58.5
7	0.1980	0.0588	70.3	0.2641	33.4	0.1709	13.7	0.1822	8.0

Table 6: Comparison with the numerical results

5.2.5   Evolution of Frequencies at Increasing Damage Level

Table 7 and Table 8 present the frequency results for the arch and the wall models for the consecutive damage tests, and Figure 12 presents the relative changes. Observing only the frequency results, it seems that the modal properties of the masonry specimens are sensitive to the damage progress. Figure 12 shows a sequential decreasing of the frequencies, with residual values in the last scenario between 0.75 and 0.90 compared to the reference values. Concerning the type of structures analyzed, this result seems to be promising, because other tests in literature report about smaller changes of the frequencies values, see [1].

Mode	Reference Test	Damage Scenario						
		I	II	III	IV	V	VI	VII
1	35.44	35.55	35.47	35.13	33.71	33.19	31.46	28.09
2	66.84	67.50	67.23	67.10	65.67	64.88	63.06	58.59
3	72.09	71.84	71.66	71.25	69.33	68.58	65.67	62.62
4	125.63	125.70	125.70	125.99	124.33	123.76	122.10	119.28
5	140.17	140.20	139.71	139.38	136.74	136.17	130.16	126.81
6	173.83	174.10	174.76	173.99	172.48	170.73	167.85	156.41
7	193.30	197.50	195.85	198.75	192.26	185.67	186.22	180.38

Table 7: Frequency results for the arch model through the different damage scenarios in Hz

Mode	Reference Test	Damage Scenario				
		XXVI	XXVII	XXVII	XXIX	XXX
1	3.53	3.40	3.41	3.39	3.00	2.81
2	12.65	12.52	12.44	11.72	10.80	9.24
3	18.62	18.31	18.22	17.57	16.74	16.00
4	35.44	35.17	35.34	34.58	33.14	32.84

Table 8: Frequency results for the arch model through the different damage scenarios in Hz
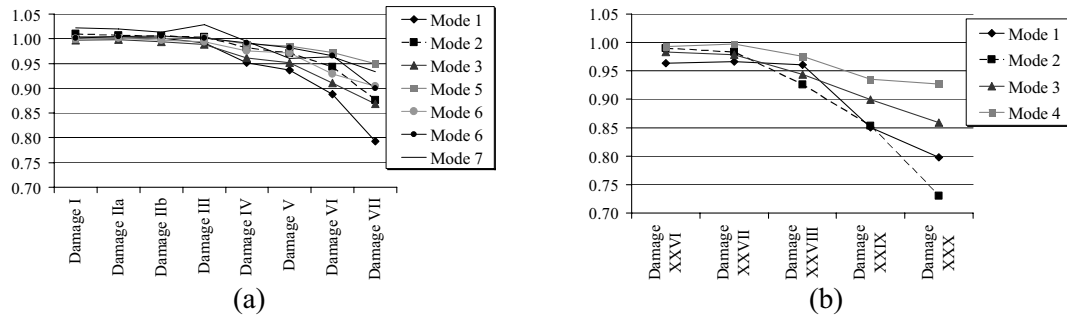

Figure 12: Relative values for the frequencies compared to the virgin state: (a) arch; and (b) wall models

In the case of the arch model a nonlinear relation can be established between the decrease of relative static stiffness of the unload branch and the relative decrease of the eigen frequencies, as can be observed in Figure 13.
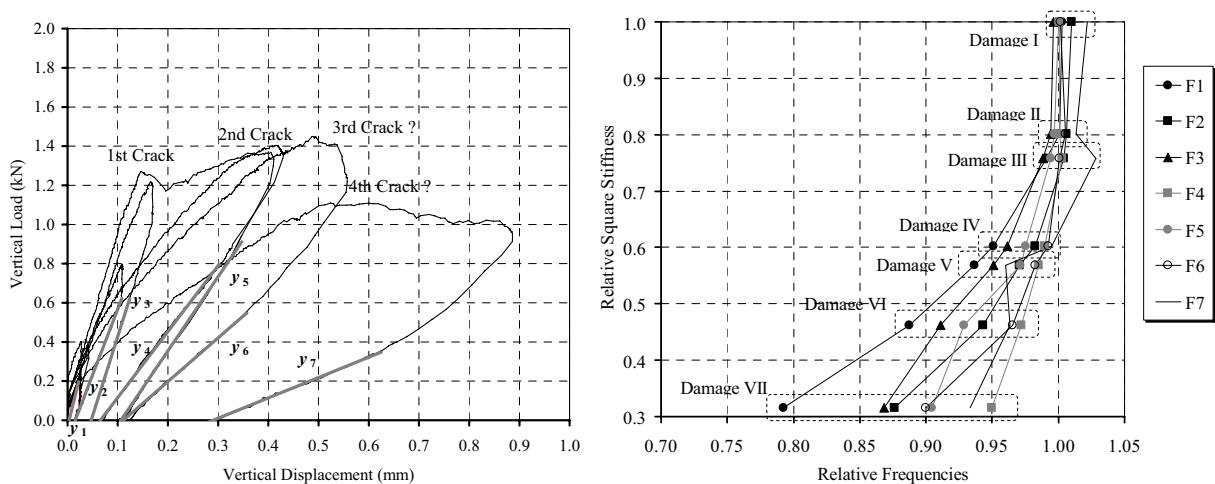

Figure 13: Stiffness decrease along the several damage scenarios

However, the results need to be further analyzed and the other modal quantities will give a better understanding about the damage progress in the structure and the efficiency of the vibrations based methods when applied to masonry structures. Special attention will be paid to the derivative quantities, such as the measured modal curvatures, because they are directly related to the local bending stiffness of

the structure. The damage identification task will be also take into account the tridimensional mode shapes and the fact that the masonry structures can, some-how, be well modeled as shell structures with out-of-plane mode shapes.

6   Preliminary Conclusions and Future Work

In the paper, a new approach for the damage identification process by using Global and Local methods in masonry structures was outlined. Vibration analysis is presented as a potential candidate for Global identification at Levels 1 and 2.

Two experiments on simple masonry structures are set up. The results of the system identification techniques show good accordance between the two SSI techniques. Any of the two implementations can be satisfactorily used for the estimation of the modal quantities of the several damage scenarios.

With the environmental tests in the laboratory it was possible to conclude that a normal variation of temperature and relative air humidity do not change the dynamic response of the specimen. Therefore, those tests assure the reliability and repetitivity of the tests.

The results emerged form the first optimization analysis show high sensitivity of the arch to the geometry. The correspondence between the numerical and the experimental results is acceptable but still some improvement will be applied in order to get even better results.

In order to be able to used damage identification methods that require scaled modes, also added masses tests were preformed in the specimen to calculate scale factors. The results are acceptable, although some differences were found between the measured and the numerical scale factors.

The preliminary results from the damage scenarios show that the modal properties of the simple masonry specimens are sensitive to the induced damage. In terms of frequency results, the low frequency values significantly decrease at progressing damage, more then reported for similar structures in literature. If this observation is confirmed with real case studies, such as buildings, bridges or towers, the vibration based damage identification techniques applied to similar masonry constructions can be a useful tool for the preservation of ancient masonry structures. However, the results of the experimental campaign need to be carefully further analyzed.

The next phase of the analysis should be the application of direct methods, such as Damage Index Method and the Direct Stiffness Calculation. In a second phase, model updating techniques will be applied.

Acknowledgements

References

[1]   S.W. Doebling, C.R. Farrar, M.B Prime, D. Shevitz, *Damage identification and health monitoring of structural and mechanical systems from changes in their vibration characteristics: a literature review*, Los Alamos National Laboratory, NM (1996).

[2]   B. Peeters, *System Identification and Damage Detection in Civil Engineering*, PhD Thesis, Catholic University of Leuven, Belgium (2000).

[3]   P.C. Chang, A. Flatau, S.C. Liu, *Review Paper: Health Monitoring of Civil Infrastructure, Structural Health Monitoring*, Vol. 2 (3), pp. 257-267 (2003).

[4] J.E. Doherty, *Nondestructive Evaluation, Handbook on Experimental Mechanics*, A.S. Kobavashi Edt., Society for Experimental Mechanics, Chapter 12 (1987).

[5] K. Worden, J.M. Dulieu-Barton, *An Overview of Intelligent Fault Detection in Systems and Structures*, Structural Health Monitoring, Vol. 3(1), pp. 85-98 (2004).

[6] A. Rytter, *Vibration Based Inspections of Civil Engineering Structures*, PhD Thesis, Department of Building Technology and Structural Engineering, university of Aalborg, Denmark (1993).

[7] C.R. Farrar, S.W. Doebling, *Damage Detection and Evaluation II – Field Applications to Large Structures, Modal Analysis and Testing*, Júlio Silva and Nuno Maia (Editors), NATO Science Series E, Vol. 363, Kluwer Academic Publishers, London, pp 345-378 (1998).

[8] O.S. Salawu, *Detection of Structural Damage through Changes in Frequency: a Review*, Engineering Structures, Vol. 19, No. 9, pp. 718-723 (1997).

[9] F.M. Hemez, S.W. Doebling, *Review and Assessment of Model Updating for Nonlinear, Transient Dynamics*, Mechanical Systems and Signal Processing, 15(1) pp. 45-74 (2001).

[10] L.F. Ramos, P.B. Lourenço, A..C. Costa, *Operational Modal Analysis for Damage Detection of a Masonry Construction*, Proc. 1th Int. Operational Modal Analysis Conference, Copenhagen, Denmark, April 24-26, 2005, pp. 495-502 (2005).

[11] D.J. Ewins, *Modal Testing, Theory, Practice and Aplication*, Second Edition, Research Studies Press LTD, Baldock, Hertfordshire, England (2000).

[12] R. Brincker, L. Zhang, P. Andresen, *Modal Identification from Ambient Responses using Frequency Domain Decomposition*, Proceedings of the 18th Internation Seminar on Modal Analysis, San Antonio, Texas, 7-10 February (2000).

[13] J. Maeck, *Damage Assessment of Civil Engineering Structures by Vibration Monitoring*, PhD Thesis, Catholic University of Leuven, Belgium (2003).

[14] A. Teughels, *Inverse Modelling of Civil Engineering Structures Based on Operational Modal Data*, PhD Thesis, Catholic University of Leuven, Belgium (2004).

[15] SVS, *ARTeMIS Extractor Pro*, Release 3.42, Structural Vibration Solutions A/S, Denmark (2004).

[16] Peeters, B. and Roeck, G. De. 1999. Reference-based stochastic subspace identification for output-only modal analysis. Mechanical Systems and Signal Processing, 13(6):855-878 (1999).

[17] M.I. Friswell, J.E. Mottershead, *Finite Element Model Updating in Structural Dynamics*, Kluwer Academic Publishers, Dordrecht, The Netherlands (1995).

[18] E. Parloo, P. Verboven, P. Guillame, M. Van Overmeire, *Sensitivity-Based Operational Mode Shape Normalization*, Mechanical Systems and Signal Processing, Vol. 16, N. 5, pp 757-767 (2002).